

LETTER TO THE EDITOR



# Structural basis of sRNA RsmZ regulation of *Pseudomonas aeruginosa* virulence

© The Author(s) under exclusive licence to Center for Excellence in Molecular Cell Science, Chinese Academy of Sciences 2023

Cell Research (2023) 33:328–330; <https://doi.org/10.1038/s41422-023-00786-3>

Dear Editor,

*Pseudomonas aeruginosa* is a ubiquitous Gram-negative opportunistic bacterium that notoriously causes infections with a high mortality rate in hospitalized patients, especially those with compromised immune systems.<sup>1</sup> *P. aeruginosa* can cause acute infections that are typically associated with the cytotoxins secreted by the type III secretion system (T3SS),<sup>2</sup> as well as chronic persistence that relies on type VI secretion system (T6SS) and biofilm formation, including those in cystic fibrosis patients.<sup>3</sup> An intercellular communication network based on cell density, quorum sensing (QS), regulates numerous gene expressions including those related to both acute and chronic virulence of *P. aeruginosa*.<sup>4</sup> The global regulatory protein of the repressor of secondary metabolites (Rsm) system in bacteria, RsmA, is found to predominantly regulate these virulence entities in *P. aeruginosa* by modulating related gene expressions at transcriptional and posttranscriptional levels.<sup>5</sup>

A non-coding small RNA (sRNA) RsmZ, whose expression is regulated by the GacS/GacA two-component system,<sup>6</sup> can sequester RsmA and antagonize its repressive function, thereby promoting downstream gene expressions associated with *P. aeruginosa* virulence.<sup>7,8</sup> Previous structural and functional studies in *Pseudomonas* genus have revealed how homodimers of RsmA and other Rsm family member proteins recognized the RsmZ GGA binding sites on two separate stems that formed a clamp shape.<sup>7,9–11</sup> In particular, two conformations in a solution of the truncated RsmZ with the first four stems in complex with three RsmE homodimers in *P. fluorescens* were derived using a combination of nuclear magnetic resonance (NMR) and electron paramagnetic resonance (EPR) spectroscopy.<sup>9</sup> Although that work revealed a cooperative mechanism of RsmE assembly on RsmZ, the architecture of full-length RsmZ and molecular mechanism of RsmZ sequestration of RsmA in the pathogenic *P. aeruginosa* remains elusive, which continues to limit our understanding of RsmZ regulation of *P. aeruginosa* virulence.

Single-particle cryo-electron microscopy (cryo-EM) can resolve structures in different conformations of biological macromolecules at near-atomic resolution.<sup>12,13</sup> Here we use cryo-EM to determine structures of the full-length RsmZ in complex with RsmA homodimers in *P. aeruginosa*. Our results elucidate the structural basis of full-length RsmZ binding to RsmA, and provide molecular insights into RsmZ regulation of *P. aeruginosa* virulence.

We first separately purified full-length RsmZ transcribed in vitro and recombinant RsmA expressed in *Escherichia coli*. Incubation of RsmA and RsmZ resulted in ribonucleoprotein (RNP) complex formation when the ratio of protein to RNA reached 4:1, as observed in electrophoretic mobility shift assay (EMSA) (Supplementary information, Fig. S1a). Additions of different detergents, including lauryl maltose neopentyl glycol (LMNG), octyl-beta-glucoside ( $\beta$ -OG) or glyco-diosgenin (GDN), facilitated more

efficient complex formation in the presence of fewer proteins, indicating that these detergents may enable the faster formation of more stable RNP complexes (Supplementary information, Fig. S1b–d).

Single-particle cryo-EM analysis of the RsmZ–A complex in the presence of GDN yielded a three-dimensional (3D) reconstruction of the full-length RsmZ in complex with three RsmA homodimers (RsmZ–A<sub>3</sub>) at 3.80 Å resolution (Fig. 1a–c; Supplementary information, Table S1 and Fig. S2). RsmZ consists of six consecutive stem loops (SLs), namely SL1–SL5 and a rho-independent terminator SL (SL<sub>ter</sub>) that controls processing of the complete RsmZ.<sup>14</sup> SL<sub>ter</sub> coaxially stacks on SL5 and points away from the rest of the complex (Fig. 1c), which is distinct from the previously predicted secondary structure.<sup>7</sup> Six GGA binding sites in the loop regions of SL1–SL5 and a single-stranded junction between SL2 and SL3 (J2/3) are grouped into three pairs, SL1 and SL5, SL2 and SL3, J2/3 and SL4. Each pair resembles a clamp shape that binds an RsmA homodimer via interactions between the GGA motifs of RsmZ and residues 36–44 of RsmA (Supplementary information, Fig. S3a–f), similar to previous truncated structures of homologous RsmZ–E in *P. fluorescens* and RsmZ–N in *P. aeruginosa* (Supplementary information, Fig. S3g–i).<sup>9,11</sup> Previous study has derived structures of truncated RsmZ with SL1–SL4 (nucleotides 1–72) bound to RsmE in *P. fluorescens* using NMR and EPR.<sup>9</sup> Sequence alignment and covariance analysis among *Pseudomonas* RsmZs revealed that SL1–SL4 and SL<sub>ter</sub> are structurally conserved between *P. aeruginosa* and *P. fluorescens* (Supplementary information, Fig. S4). However, comparisons of the full-length and truncated RsmZs reveal substantially different architectures, with only one of the RsmA binding clamps, consisting of SL2 and SL3 in both RsmZs, interacting with RsmA homodimer in a similar way (Supplementary information, Fig. S5).

Another state of the RsmZ–A complex with one RsmA homodimer missing between SL2 and SL3 was isolated from 3D classification (Supplementary information, Fig. S6a). The superposition of RNP structures with two or three RsmA homodimers reveals a  $\sim 6.2^\circ$  rotation of SL<sub>ter</sub> (Supplementary information, Fig. S6b), indicating the dynamics of SL<sub>ter</sub> during RsmA binding, which is also supported by the local resolution map (Supplementary information, Fig. S2b, c).

Previous studies observed sequential and cooperative bindings of RsmE to RsmZ in *P. fluorescens*, in which binding affinity was affected by the sequence of the loop and closing base pairs of the stem.<sup>9,10</sup> Here we observed the formation of RsmZ predominantly in complex with three RsmA homodimers with trace amounts of intermediate complexes in EMSA, indicative of cooperative binding of RsmA homodimers to RsmZ similar to previously reported binding of RsmZ to RsmE (Supplementary information, Fig. S1). To evaluate the critical roles that RsmZ structure plays in RsmA binding in *P. aeruginosa*, we first determined the

Received: 5 November 2022 Accepted: 6 February 2023  
Published online: 24 February 2023

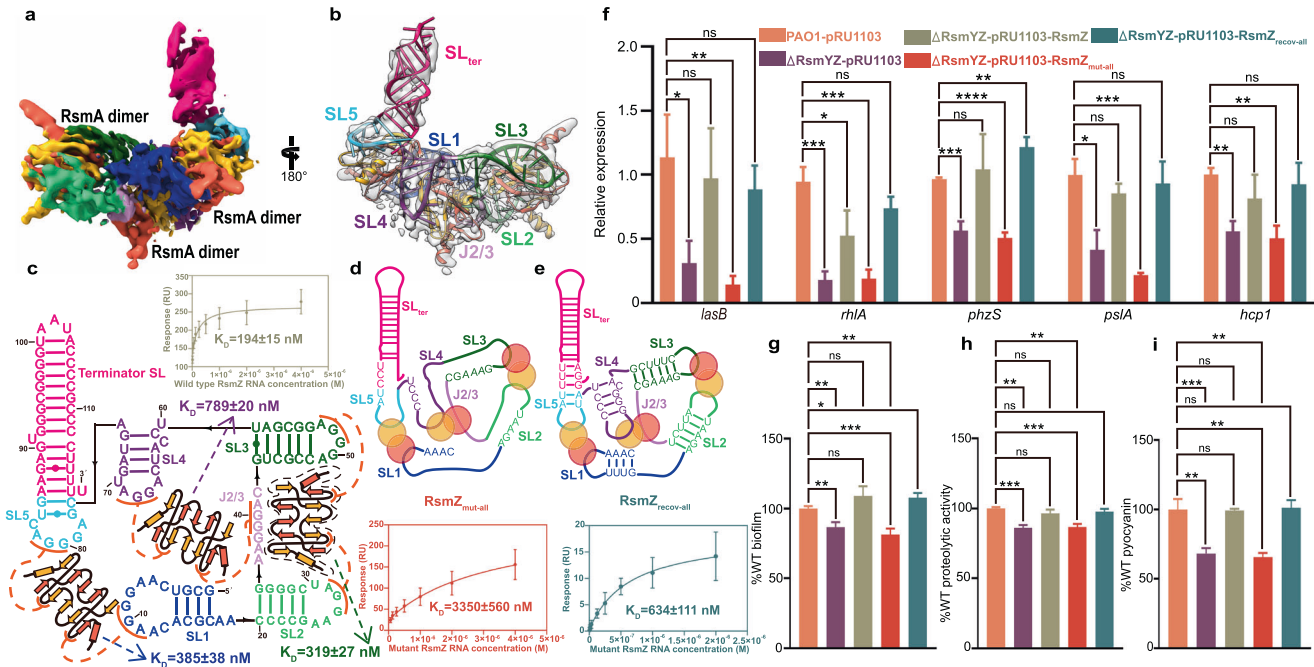


**Fig. 1** Cryo-EM structures, RsmA binding affinity and regulation of WT and mutant RsmZ on gene expressions and phenotypes associated with *P. aeruginosa* virulence. **a** The segmented map of RsmZ in complex with three RsmA homodimers colored according to the secondary structure. **b** Cryo-EM map and colored model of RsmZ in complex with three RsmA homodimers. **c** Secondary structure of the RsmZ–A cryo-EM model and binding affinities of RsmA to the entire WT RsmZ and individual binding site. **d, e** Binding affinities of RsmA to RsmZ<sub>mut-all</sub> (**d**) and to RsmZ<sub>recov-all</sub> (**e**). Mutations introduced in RsmZ<sub>mut-all</sub> and RsmZ<sub>recov-all</sub> are shown. **f** Expression of *lasB* (elastase), *rhlA* (rhamnolipid production), *phzS* (pyocyanin), *psIA* (biofilm) and *hcp1* (H1-T6SS) genes was determined by qRT-PCR. Data shown are means  $\pm$  SD of three independent replicates. One-way ANOVA. ns,  $P > 0.05$ ; \* $P < 0.05$ ; \*\* $P < 0.01$ ; \*\*\* $P < 0.001$ ; \*\*\*\* $P < 0.0001$ . **g** Regulation of RsmZ on *P. aeruginosa* biofilm formation. Biofilm was measured by crystal violet staining and values were normalized to WT PAO1. **h** Regulation of RsmZ on *P. aeruginosa* proteolysis. Diameter values of proteolytic rings in the M9-skim milk plate were normalized to WT PAO1. **i** Regulation of RsmZ on *P. aeruginosa* pyocyanin production. Pyocyanin was detected after *P. aeruginosa* was cultured in LB medium and normalized to WT PAO1. WT PAO1 with empty pRU1103 is colored in orange, RsmYZ knockout PAO1 with empty pRU1103 in purple, and RsmYZ knockout PAO1 with different RsmZ constructs colored the same as in the binding curves (**c–e**).

dissociation constant ( $K_D$ ) of RsmZ binding to RsmA as  $194 \pm 15$  nM by surface plasma resonance (SPR) (Fig. 1c). Mutations that disrupted all five stems in RsmZ (RsmZ<sub>mut-all</sub>), including three base pairs in SL<sub>ter</sub> that stack on and stabilize SL5, led to the  $K_D$  of  $3350 \pm 560$  nM, decreased by 17-fold (Fig. 1d), whereas double mutations that recovered all stems (RsmZ<sub>recov-all</sub>) rescued the binding affinity to RsmA with the  $K_D$  of  $634 \pm 111$  nM (Fig. 1e). Individual  $K_D$  for each binding site to one RsmA homodimer upon mutations of the rest of the GGA sequences was determined as  $385 \pm 38$  nM for SL1 and SL5,  $319 \pm 27$  nM for SL2 and SL3, and  $789 \pm 20$  nM for J2/3 and SL4, respectively (Fig. 1c; Supplementary information, Fig. S7).

Non-coding sRNAs RsmY and RsmZ bind to RsmA to regulate downstream gene expression related to *P. aeruginosa* virulence.<sup>15</sup> Compared to wild-type (WT) *P. aeruginosa* reference isolate PAO1, RsmY and RsmZ double knockout mutant ( $\Delta$ RsmYZ) showed decreased expression levels of *psIA* that controls biofilm formation, *lasB*, *rhlA* and *phzS* that characterize QS activity, and *hcp1* associated to H1-T6SS (Fig. 1f), leading to compromised biofilm formation and production of QS-controlled extracellular proteases and pyocyanin (Fig. 1g–i). Expression of WT full-length RsmZ in PAO1 $\Delta$ RsmYZ restored the gene expressions and the corresponding phenotypes back to the levels comparable to those of WT PAO1, whereas expression of RsmZ<sub>mut-all</sub> with disrupted base pairings in SL1–SL5 of RsmZ in PAO1 $\Delta$ RsmYZ did not significantly change gene expressions and phenotypes of PAO1 $\Delta$ RsmYZ, due to the diminished binding of RsmZ<sub>mut-all</sub> to RsmA. Expression of RsmZ<sub>recov-all</sub> with double mutations that recovered base pairings in SL1–SL5 of RsmZ in PAO1 $\Delta$ RsmYZ rescued the gene expressions and phenotypes comparable to those of WT PAO1, consistent with the

restored binding affinity of RsmZ<sub>recov-all</sub> to RsmA (Fig. 1f–i). This suggests a RsmZ regulation mechanism through binding to RsmA, and demonstrates the critical role that RsmZ structure plays in regulation of *P. aeruginosa* virulence.

Bacterial sRNAs participate in various important biological processes such as transcription, translation, and catalysis. RsmZ in *P. aeruginosa* has been found to regulate gene expressions by sequestration of the RsmA protein, a homolog of carbon storage regulator A (CsrA) that globally regulates gene expression levels related to metabolism, QS, and virulence.<sup>15</sup> Although NMR combined with EPR provided structural insights into truncated RsmZ binding to RsmE in *P. fluorescens*,<sup>9</sup> the full-length RsmZ–A complex structure in *P. aeruginosa* remains unknown, limiting our understanding of the essential role that RsmZ structure plays in RsmA sequestration and gene expression regulations.

Recent advances in single-particle cryo-EM analysis allowed structure determination of RNAs and RNPs.<sup>12</sup> We resolved cryo-EM structures of the full-length RsmZ in complex with two or three RsmA homodimers, and revealed the global architecture of RsmZ distinct from either conformation of the truncated RsmZ in *P. fluorescens* (Fig. 1a, b; Supplementary information, Fig. S5). Binding experiments suggested cooperative binding of RsmZ to three RsmA homodimers similar to the binding of RsmZ to RsmE.<sup>9</sup> Disruptions of all stems enclosing each binding site in RsmZ significantly decreased binding affinity to RsmA, which was recovered by double mutations that restored base pairing of all stems, suggesting that the entire stem containing the SL enclosing base pairs has an impact on protein binding of RsmZ (Fig. 1c–e).<sup>10</sup> Subsequent functional experiments demonstrated that maintaining the intact RsmZ architecture is crucial for regulating gene expression and the corresponding phenotypes

related to QS, T6SS and biofilm formation associated with *P. aeruginosa* virulence (Fig. 1f–i). The overall conserved sequences and structures of *Pseudomonas* RsmZ suggest a universal protein sequestration mechanism regulated by the RsmZ structure (Supplementary information, Fig. S4). Together, our results provide the structural basis of RsmA sequestration by RsmZ, and establish the critical role of sRNA architecture in regulations of *P. aeruginosa* virulence, which may facilitate novel RNA-targeted antimicrobial development.

Xinyu Jia<sup>1,6</sup>, Zhiling Pan<sup>1,6</sup>, Yang Yuan<sup>2,6</sup>, Bingnan Luo<sup>1</sup>,  
Yongbo Luo<sup>1</sup>, Sunandan Mukherjee<sup>3</sup>, Guowen Jia<sup>1</sup>,  
Liu Liu<sup>4</sup>, Xiaobin Ling<sup>1</sup>, Xiting Yang<sup>2</sup>, Zhichao Miao<sup>5</sup>,  
Xiawei Wei<sup>1</sup>, Janusz M. Bujnicki<sup>3</sup>, Kelei Zhao<sup>2</sup>✉ and  
Zhaoming Su<sup>1</sup>✉

<sup>1</sup>The State Key Laboratory of Biotherapy, Department of Geriatrics and National Clinical Research Center for Geriatrics, West China Hospital, Sichuan University, Chengdu, Sichuan, China. <sup>2</sup>Antibiotics Research and Re-evaluation Key Laboratory of Sichuan Province, School of Pharmacy, Chengdu University, Chengdu, Sichuan, China. <sup>3</sup>Laboratory of Bioinformatics and Protein Engineering, International Institute of Molecular and Cell Biology in Warsaw, ul. Ks. Trojdena 4, PL-02-109, Warsaw, Poland. <sup>4</sup>Department of Conservative Dentistry and Endodontics, West China Hospital of Stomatology, Sichuan University, Chengdu, Sichuan, China. <sup>5</sup>Guangzhou Laboratory, Guangzhou International Bio Island, Guangzhou, Guangdong, China. <sup>6</sup>These authors contributed equally: Xinyu Jia, Zhiling Pan, Yang Yuan. ✉email: zhaokelei@cdu.edu.cn; zsu@scu.edu.cn

#### DATA AVAILABILITY

The cryo-EM maps and associated atomic coordinate models of the complete RsmZ–A complex have been deposited in the wwPDB OneDep System under EMD accession code EMD-34048 and PDB ID code 7YR7, and the RsmZ–A complex with one missing RsmA homodimer in the wwPDB OneDep System under EMD accession code EMD-34047 and PDB ID code 7YR6.

#### REFERENCES

1. Kang, C.-I. et al. *Clin. Infect. Dis.* **37**, 745–751 (2003).
2. Hauser, A. R. *Nat. Rev. Microbiol.* **7**, 654–665 (2009).
3. Høiby, N., Ciofu, O. & Bjarnsholt, T. *Future Microbiol.* **5**, 1663–1674 (2010).
4. Lee, J. & Zhang, L. *Protein Cell* **6**, 26–41 (2015).
5. Goodman, A. L. et al. *Dev. Cell* **7**, 745–754 (2004).
6. Brenic, A. et al. *Mol. Microbiol.* **73**, 434–445 (2009).
7. Janssen, K. H. et al. *J. Bacteriol.* **200**, e00736–17 (2018).
8. Papenfert, K. & Vogel, J. *Cell Host Microbe* **8**, 116–127 (2010).

9. Duss, O. et al. *Nature* **509**, 588–592 (2014).
10. Duss, O., Michel, E., Diarra dit Konté, N., Schubert, M. & Allain, F. H.-T. *Nucleic Acids Res.* **42**, 5332–5346 (2014).
11. Morris, E. R. et al. *Structure* **21**, 1659–1671 (2013).
12. Ma, H., Jia, X., Zhang, K. & Su, Z. *Signal. Transduct. Target. Ther.* **7**, 58 (2022).
13. Chua, E. Y. D. et al. *Annu. Rev. Biochem.* **91**, 1–32 (2022).
14. Heeb, S., Blumer, C. & Haas, D. *J. Bacteriol.* **184**, 1046–1056 (2002).
15. Vakulskas, C. A., Potts, A. H., Babitzke, P., Ahmer, B. M. M. & Romeo, T. *Microbiol. Mol. Biol. Rev.* **79**, 193–224 (2015).

#### ACKNOWLEDGEMENTS

Cryo-EM data were collected on Can Cong at SKLB West China Cryo-EM Center and processed at Duyu High Performance Computing Center in Sichuan University. This work was supported by the Ministry of Science and Technology of China (2022YFC2303700 and 2021YFA1301900 to Z.S.), the National Natural Science Foundation of China (32222040 and 32070049 to Z.S., 31970131 to K.Z.), and Sichuan University start-up funding (20822041D4057 to Z.S.); J.M.B. and S.M. were supported by the Polish National Science Center (NCN 2017/26/A/NZ1/01083 and NCN 2021/43/D/NZ1/03360, respectively). Computational resources for SimRNA simulations were provided by the Poznań Supercomputing and Networking Center at the Institute of Bioorganic Chemistry, Polish Academy of Sciences through the Polish Grid Infrastructure (grant: plgsimcryox). Z.M. was supported by R&D program of Guangzhou Laboratory (SRPG22-003).

#### AUTHOR CONTRIBUTIONS

Z.S. conceived the project. X.J., Z.P. and G.J. prepared RNAs and proteins. X.J. constructed expression plasmids. X.J., Z.P. and X.L. performed binding experiments. Y.Y., X.Y., X.W. and K.Z. carried out phenotype and qRT-PCR experiments. Y.L. collected cryo-EM data. Y.L., X.J. and B.L. processed cryo-EM data. X.J., B.L., S.M. and J.M.B. built and refined atomic models. L.L. carried out covariation analysis of RsmZ secondary structure and sequence alignment. All authors contributed to the preparation of the manuscript.

#### COMPETING INTERESTS

The authors declare no competing interests.

#### ADDITIONAL INFORMATION

**Supplementary information** The online version contains supplementary material available at <https://doi.org/10.1038/s41422-023-00786-3>.

**Correspondence** and requests for materials should be addressed to Kelei Zhao or Zhaoming Su.

**Reprints and permission information** is available at <http://www.nature.com/reprints>